



Cite this: *J. Anal. At. Spectrom.*, 2015, **30**, 1655

Improved plutonium concentration analysis in specimens originating from the nuclear fuel cycle using high resolution ICP-OES

Michael Krachler* and Rafael Alvarez-Sarandes

An accurate and robust ICP-OES procedure for the reliable determination of the Pu concentration in radioactive samples was developed and subsequently cross-validated using ICP-MS. Method optimisation focused on identifying Pu emission wavelengths that are spectrally not interfered by the occurrence of emission signals of concomitant elements (e.g. Am, Np, Th, and U) in the analyte solution, thereby avoiding an otherwise necessary chemical separation of Pu from the matrix elements. To this end, a total of 43 Pu emission wavelengths were tested for their selectivity and sensitivity. The signal to background ratio of the 27 most prominent Pu emission lines ranged from ~ 2 to 20, while relative sensitivities varied only within a factor of two. Peak widths of ICP-OES Pu signals extended from ~ 5 pm to ~ 11 pm, with the majority remaining < 6 pm. Using a desolvating nebuliser, instrumental detection limits (LOD) were lowered by an order of magnitude compared to all previous studies. Among the finally selected, seven worthwhile Pu emission wavelengths, LODs of $2.3 \mu\text{g L}^{-1}$, $3.1 \mu\text{g L}^{-1}$, and $3.2 \mu\text{g L}^{-1}$ were obtained at $\lambda = 299.649$ nm, $\lambda = 299.409$ nm, and $\lambda = 297.251$ nm. Applying external calibration, several radioactive samples originating from pyrochemical separation experiments were analysed for their Pu concentration. Typical relative standard deviations of replicate Pu measurements amounted to $\sim 1\%$ to 2% . The complementary employment of the standard addition approach confirmed the accuracy of this data as well did comparative in-house sector field ICP-MS analysis. Preliminary experiments with spent fuel solutions revealed promising Pu data highlighting the potential of ICP-OES for reliable Pu analysis in the nuclear field.

Received 22nd May 2015
Accepted 3rd June 2015

DOI: 10.1039/c5ja00187k

www.rsc.org/jaas

Introduction

Even though plutonium (Pu) has been present in the universe ever since the first supernova occurred about 100 000 years after the Big Bang,¹ Pu is principally considered a man-made element. During the last few decades substantial amounts (~ 1300 tonnes) of Pu have also been produced as a by-product during the operation of uranium-driven nuclear reactors all over the globe.² Of course, Pu is also a major component of various nuclear weapons. Because Pu is a highly toxic, radioactive, fissile element, its use is strictly controlled by national and international safeguard programmes.³

Mass spectrometric techniques such as ICP-MS, MC-ICP-MS, accelerator mass spectrometry (AMS) and TIMS, but also alpha and gamma spectrometry, are commonly used to determine both Pu concentrations and the abundance of various Pu isotopes.^{4–7} These instrumental techniques normally require a chemical separation of Pu from U (e.g. via liquid–liquid extraction using TBP (tri-*n*-butyl phosphate) or using

commercial pre-packed columns such as TEVA) to reduce detrimental interferences that would otherwise hamper the reliable determination of specific Pu isotopes. The quantification of ^{238}Pu using ICP-MS, for example, suffers from the isobaric spectral interference of ^{238}U (99.275% natural abundance), while the formation of ^{238}UH deteriorates the reliable analysis of ^{239}Pu by mass spectrometry.^{4–7} Similarly, the presence of ^{241}Am in a sample complicates the mass spectrometric measurement of the ^{241}Pu . In alpha spectrometry, in turn, the signals of ^{239}Pu and ^{240}Pu occur as a single peak because both isotopes have similar energies which often cannot be discriminated sufficiently.^{4,6} All these constraints hamper reliable Pu concentration analyses, which comprises the sum of the contributions of all individual Pu isotopes.

The disadvantageous analytical effects described above may be overcome using ICP-OES if sufficiently sensitive Pu emission wavelengths are identified that do not overlap with spectral lines arising from other concomitant elements present in the sample to be analysed. In fact, being aware of the limitations of α - and γ -spectrometry, Claudon *et al.*⁸ investigated the impact of the presence of Am and U in the analyte solution on various prominent Pu emission wavelengths employing ICP-OES already almost three decades ago. Due to the low optical

European Commission – Joint Research Centre, Institute for Transuranium Elements, P.O. Box 2340, D-76125 Karlsruhe, Germany. E-mail: michael.krachler@ec.europa.eu; Web: <http://www.itu.jrc.ec.europa.eu>; Fax: +49 7247 951 588; Tel: +49 7247 951 884



resolution of 20 pm of their employed ICP-OES, only the Pu emission wavelength at $\lambda = 453.62$ nm was recommended for Pu analysis.⁸ Later, Kulkarni *et al.*⁹ studied the influence of the presence of U and Th on two prominent Pu ICP-emission wavelengths. Already at a 10-fold excess of either U or Th, the Pu emission signal at $\lambda = 300.06$ nm yielded distinctly elevated Pu concentrations.⁹ The Pu emission signal at $\lambda = 453.62$ nm, in turn, was found to be free from these spectral interferences.⁹ More recently, the spectral performance of the two above mentioned Pu emission wavelengths was tested using a high resolution (HR-)ICP-OES instrument.¹⁰ Employing experimentally established inter-elemental correction factors, the potential impact of a 10-fold excess of U, Th and selected rare earth elements was limited to an increase of 8% with respect to the target Pu concentration.¹⁰

Despite several earlier investigations,^{8–10} the potential of HR-ICP-OES for the reliable determination of Pu in nuclear specimens is not yet fully exploited. While most previous studies focussed on only a few Pu emission wavelengths, the current study investigates as many as 43 of them aiming at arriving at a list of sensitive Pu emission wavelengths that works reliably with genuine samples. This endeavour also includes setting up measures to lower Pu detection limits (LOD) compared to values reported in the current scientific literature. Specific emphasis is targeted on the identification of wavelengths that do not suffer from spectral interferences and thus do neither need correction factors to be applied nor a chemical separation prior to Pu analysis. Altogether, this study attempts to develop an analytical procedure allowing the reliable, simple and fast quantification of Pu in samples related to the nuclear fuel cycle using HR-ICP-OES.

Experimental

Instrumentation

All measurements were carried out with a commercial high resolution (HR-)ICP-OES instrument (Ultima2, HORIBA Jobin Yvon, Longjumeau, France). The entire sample introduction system including the autosampler (AS500, HORIBA) of this sequentially working optical spectrometer was installed in a glove box enabling the analysis of the radioactive samples. This demanding adaptation of the original ICP-OES set-up protected the analyst from α and β radiation of the sample solutions to be analysed. A PolyPro ST nebuliser (Elemental Scientific, Inc., Omaha, NE, USA) was attached to a high efficiency sample introduction system (Apex E, Elemental Scientific) enhancing ICP-OES performance. The ICP was operated at 1000 W forward power. More detailed operating and data acquisition parameters of the HR-ICP-OES are reported elsewhere.^{11,12}

For quality assurance selected samples and the Pu stock solution used for calibrating the ICP-OES response were additionally analysed for their Pu concentration in-house using sector field (SF-)ICP-MS (Element2, Thermo Scientific). Similar to the ICP-OES set-up, a glove box hosted the sample introduction system of the SF-ICP-MS that was run under routine conditions according to accredited standard operating procedures.

Reagents and standards

High purity water (18.2 M Ω cm) from a Milli-Q Element (Millipore) water purification system and sub-boiled nitric acid were used for the preparation of all solutions.

Because of their radioactive nature, all investigated samples were handled in appropriate glove boxes following strict safety and security procedures. As such, all analysed samples had to be bagged-in into a dedicated glove box through a lock system prior to any measurement. To minimise the radioactive dose to the operator, samples were fed to the sample introduction system of the ICP-OES with an autosampler.

A concentrated Pu solution was prepared by dissolving a piece of Pu metal (~ 0.55 g; Pu content: $99.90 \pm 0.04\%$) in hydrochloric acid as recommended by the supplier of this reference material (Plutonium Metal “MP2”, CETAMA, CEA VALHRO, Marcoule, France). A 100 mg kg⁻¹ working stock solution was obtained by diluting an aliquot of the concentrated Pu solution with 8 M nitric acid using an analytical balance. The purity and actual Pu concentration of this working stock standard solution was confirmed by in-house SF-ICP-MS analysis. Seven Pu solutions with nominal Pu concentrations of 0, 150, 350, 500, 650, 850, and 1000 $\mu\text{g kg}^{-1}$ in 0.14 M HNO₃ were prepared for setting up calibration curves at all investigated Pu emission wavelengths.

Additional standard addition experiments involved the analysis of the actual sample plus three spiked sample aliquots with increasing Pu concentrations. All solutions were prepared on a weight basis to avoid inaccuracies related to the delicate handling of small volumes with pipets inside the glove box.

For the interference study, single element solutions of natural U and Th (prepared from 1000 mg kg⁻¹ stock solutions, Specpure®, Alfa Aesar) in 1 M nitric acid as well as thoroughly characterised ²⁴¹Am and ²³⁷Np solutions (prepared and characterised in-house)^{12–14} were employed.

Radioactive samples

Pyrochemical actinide partitioning. The analysed samples originated from in-house pyrochemical experiments focussing on the homogeneous recovery of all actinides from metallic nuclear fuels.¹⁵ Briefly, the fuel was dissolved anodically in a molten salt consisting of a LiCl-KCl eutectic mixture. Salt samples generated throughout this process were subsequently dissolved in a mixture of 1 M HNO₃, 0.1 M HF and 1 M HCl. For analysis in the present study, all solutions were diluted with 0.14 M HNO₃. Details of the experimental procedure as well as the preparation and nature of the investigated nuclear samples can be found elsewhere.^{12,15}

Spent fuel. Two different kinds of spent fuel were considered for this study. All corresponding solutions were diluted gravimetrically. First, a two mm slice of an irradiated (Th, Pu)O₂ fuel rod was dissolved by boiling under reflux in a so-called “Thorex solution” containing Al(NO₃)₃·9H₂O, NaF and 14.4 M HNO₃ in a chemical hot-cell at JRC-ITU using telemanipulators within the framework of a Th irradiation project called *LWR-Deputy*.¹⁶ The dissolved fuel solution was further diluted ~ 200 times with 0.14 M nitric acid for subsequent ICP-OES analysis.



Similarly, a metallic fuel, irradiated in the frame of the *METAPHIX-1 Project*,¹⁷ was dissolved and investigated for its Pu concentration. The experimental research fuel has been doped with 2% rare earth elements and 2% minor actinides in order to study the impact of irradiation on these elements. The dissolution of the fuel samples was carried out by boiling under reflux in a mixture of 3 M HNO₃ and 0.2 M HF in a chemical hot-cell at JRC-ITU. From these dissolved fuel solutions, further sample dilutions (~4000 times) have been prepared using 0.14 M HNO₃ for ICP-OES analysis.

Results and discussion

Selection of wavelengths

Because the recent scientific literature is lacking a compilation of suitable, sensitive ICP-OES emission wavelengths for Pu, all 43 wavelengths available in the instrument software were tested for potential Pu analysis. To this end, emission spectra centred around the reported Pu peak maxima were recorded within a distance of ± 50 pm in 1 pm increments aspirating a 1 mg kg⁻¹ Pu solution. In addition, spectra of a blank solution containing 0.14 M HNO₃ were investigated at the above mentioned wavelength regions aiming at identifying non-Pu-specific emission signals. After this initial screening, the use of 16 Pu emission wavelengths was no longer pursued because they were either of low sensitivity or consisted of unfavourable peak shapes and/or a noisy spectral background.

Subsequently the remaining 27 Pu wavelengths were investigated in more detail, specifically for their sensitivity, selectivity and detection limits.

Spectroscopic characterisation of Pu emission lines

These 27 most promising Pu emission wavelengths are listed in chronological order in Table 1, together with some relevant spectroscopic characteristics. The first ten wavelengths from $\lambda = 292.555$ nm to $\lambda = 300.057$ nm provide the best signal-to-background (*S/B*) ratio, while starting from $\lambda = 319.844$ nm *S/B* ratios clearly deteriorate. It should be noted, however, that these values reveal a day-to-day variability of approximately $\pm 10\%$. A similar trend holds true for the slope of the calibration curves (Table 1), as exemplified for three selected Pu emission wavelengths in Fig. 1. However, as indicated by the relative sensitivity of the tested 27 emission wavelengths, the spread between the most and the least sensitive emission line is only a factor of about two (Table 1). In other words, sensitivity issues are not the main selection criteria for a specific wavelength because the instrumental response of all investigated Pu wavelengths is comparable within a factor of two.

In this respect, the ICP-OES performance of Pu is similar to that of Am, but it is in large contrast to the spectroscopic behaviour of other actinides such as Np and U.^{12,13,18} While relative sensitivities of up to ~30 were established recently for Np at the most sensitive emission wavelengths,¹² for Am corresponding maximum values amounted to only ~1.8.¹³ Similarly, *S/B* ratios of up to ~30 were achievable for U,¹⁸ numbers that are slightly superior to those of Pu (Table 1).

The peak width (full width at half maximum, FWHM) of most of the tested Pu emission signals range from ~5 to ~6 pm (Table 1). However, also broad peaks having widths of up to ~11 pm are found, particularly at higher emission wavelengths. In general, narrower signals are preferred for data evaluation because they often provide a superior *S/B* ratio as well as a higher relative sensitivity (Table 1). In addition, the narrower the peak, the less likely is the occurrence of spectral interferences that might hamper the reliable determination of the analyte, *i.e.* Pu. One exception in this context, however, is the Pu emission signal at $\lambda = 453.615$ nm being broad and also offering high sensitivity at the same time. If peak area is considered for data evaluation, this constellation could lead to substantial performance improvement at this particular Pu emission wavelength. The software of the employed ICP-OES instrument, however, supports only peak height measurements, leaving this option untouched.

While the typical peak width of Pu emission signals acquired with the employed ICP-OES instrument is <6 pm, it can be as large as ~11 pm. For U representative peak widths are ~4 pm,¹⁸ while those of other actinides such as Am and Np range from ~3–12 pm (ref. 13) and ~4–30 pm (ref. 12), respectively. In this context, the spectroscopic behaviour of Pu is similar to that of the minor actinides Am and Np.

Analytical performance

Prior to the assessment of instrumental detection limits (LOD), the detector voltage (final range: 774–955 V) for each Pu emission wavelength was optimised using a 1 mg kg⁻¹ Pu solution. This experimental approach established the optimum compromise between sensitivity, spectral baseline and the corresponding *S/B* ratio. Detection limits for Pu were computed based on the results of 25 measurements of a blank solution containing 0.14 M HNO₃. To this end, the signal intensity of the 25 blank measurements was averaged for each wavelength. Subsequently, the LOD was calculated as the concentration corresponding to three times the standard deviation of this blank (3σ criterion).

An exhaustive list comprising the LOD obtained at each of the 27 investigated Pu emission wavelengths is given in Table 2. This record represents by far the most comprehensive collection of Pu emission wavelengths and corresponding Pu LOD in the recent scientific literature. To put the data of the current study into perspective and for a sound comparison, previously reported Pu LOD are additionally summarised in Table 2. Depending on both the selected Pu emission wavelength and study, best Pu LOD reported formerly range from 15 to 100 $\mu\text{g L}^{-1}$ (Table 2). Interestingly, achievable LOD at a particular wavelength vary considerably. At the Pu emission wavelength $\lambda = 300.057$ nm (one of the most frequently selected Pu emission wavelengths), for example, Mainka *et al.*¹⁹ achieved the lowest Pu LOD of 20 $\mu\text{g L}^{-1}$, while higher values of 28 $\mu\text{g L}^{-1}$, 30 $\mu\text{g L}^{-1}$, 54 $\mu\text{g L}^{-1}$, 100 $\mu\text{g L}^{-1}$ and 200 $\mu\text{g L}^{-1}$ have been reported by other authors.^{8–10,19–21} This diversity in Pu LOD reflects, beside other issues, the different sensitivity of the employed detectors across the studied wavelength region.



Table 1 Spectroscopic characteristics of the 27 most prominent Pu emission lines as determined using HR-ICP-OES

Wavelength [nm]	Signal/background	Slope ^a	Relative sensitivity ^b	Peak width [pm]
292 555	10.6	84 240	1.7	5.8
293 912	11.8	95 590	2.0	5.1
295 005	14.9	95 970	2.0	5.0
295 455	11.1	90 460	1.9	6.0
296 464	11.6	85 290	1.8	5.8
297 251	15.9	88 450	1.8	5.3
298 023	10.2	94 160	2.0	5.3
299 409	15.1	94 590	2.0	6.8
299 649	19.6	92 570	1.9	5.2
300 057	18.5	103 440	2.1	5.6
319 844	3.3	68 430	1.4	5.7
340 110	6.6	81 410	1.7	5.2
346 510	5.2	75 070	1.6	4.8
358 587	5.7	74 160	1.5	5.1
363 221	6.5	76 940	1.6	9.3
390 721	4.4	81 740	1.7	5.7
397 220	2.7	57 570	1.2	5.3
397 543	3.1	60 610	1.3	5.7
402 154	3.3	48 500	1.0	4.6
435 271	2.6	66 220	1.4	8.2
437 990	1.7	48 280	1.0	10.0
439 645	2.6	63 560	1.3	8.4
447 270	2.7	67 090	1.4	10.5
449 378	3.0	71 920	1.5	8.3
450 492	3.1	76 870	1.6	8.3
453 615	6.8	93 420	1.9	9.0
476 717	2.0	52 110	1.1	7.9

^a Net intensity (counts) per mg kg⁻¹ Pu. ^b Normalised to the emission intensity obtained at $\lambda = 437.990$ nm.

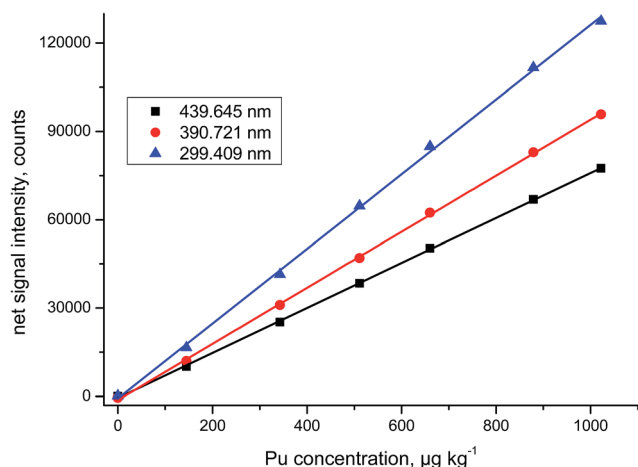


Fig. 1 Representative Pu calibration curves up to a concentration of 1 mg kg⁻¹ at three selected prominent Pu emission wavelengths, *i.e.* $\lambda = 299.409$ nm, $\lambda = 390.721$ nm, and $\lambda = 439.645$ nm. Correlation coefficients of these regression curves are always >0.999, but absolute values of their slopes might vary up to 10% on a day-to-days basis. Relative standard deviations of replicate measurements ($N = 3$) of single calibration points are <2%.

It is important to stress that the vast majority of Pu LOD determined in the current study at any emission wavelength is lower than the best LOD reported before for optimum Pu

wavelengths (Table 2). In general, LOD presented here were improved by about an order of magnitude compared to earlier work, including other studies employing the same ICP-OES model used in the current study.¹⁰ In fact, the two emission wavelengths $\lambda = 300.057$ nm and $\lambda = 453.615$ nm considered in this latter study¹⁰ yielded LOD for Pu of 30 µg L⁻¹ (*vs.* 2.2 µg L⁻¹ in the current investigation) and 70 µg L⁻¹ (10 µg L⁻¹), respectively. This difference in LOD can be partly explained by the different nebulisers used in the two studies, *i.e.* pneumatic nebuliser (Meinhard TR 50-C1 made from glass)¹⁰ operated at 1 mL min⁻¹ *vs.* a low flow nebuliser (PolyPro ST made from polypropylene) in combination with a desolvator aspirating 0.3 mL of sample solution min⁻¹ in this study.

Compared to previous work the use of the low flow nebuliser allowed for a 3-fold reduction of the sample volume required for analysis in the current work, producing less radioactive waste that is expensive to dispose of.

Spectral interferences

One of the potential benefits of ICP-OES over ICP-MS for Pu analysis of nuclear samples is the fact that no chemical separation of the actinide from matrix elements might be required when using ICP-OES. If doable, this advantage obviously speeds up the analysis and thereby reduces the waste amounts and also lowers the radiation dose to the analyst. Excess amounts of U



Table 2 Comparison of Pu limits of detection [$\mu\text{g L}^{-1}$] obtained at various ICP-OES emission lines as reported by several authors^a

Wavelength [nm]	Limit of detection, LOD				
	This study	Ref. 21	Ref. 8	Ref. 19	Ref. 20
292 555	2.9	—	—	—	—
293 912	3.2	—	—	—	—
295 005	2.5	46	250	104	76
295 455	3.0	—	—	—	—
296 464	6.2	61	200	108	61
297 251	3.2	29	100	19	68
298 023	2.1	52	—	51	122
299 409	3.1	48	—	—	57
299 649	2.3	30	150	35	81
300 057	2.2	28	100	20	54
319 844	11	167	—	456	81
340 110	9.0	78	—	403	50
346 510	20	—	—	—	—
358 587	35	—	—	—	—
363 221	7.3	49	300	51	25
390 721	5.5	—	—	—	—
397 220	15	—	—	—	—
397 543	8.2	—	—	—	—
402 154	12	—	—	—	—
435 271	9.7	—	—	—	—
437 990	20	—	—	—	—
439 645	14	—	—	—	—
447 270	9.4	—	—	—	—
449 378	11	—	—	—	—
450 492	10	—	—	—	—
453 615	10	89	220	—	15
476 717	18	—	—	—	—

^a Limit of detection, based on the 3σ criterion. See text for details.

frequently present in spent nuclear fuel solutions, for example, create a huge ICP-MS response in the mass spectrum at m/z 238 that spills over into the much smaller Pu signal at m/z 239. In addition, the formation of the polyatomic ^{238}UH species always adds to the ^{239}Pu signal in mass spectrometry and therefore needs to be corrected for.^{5,6} Consequently, Pu determinations employing mass spectrometry require utmost attention and in addition, frequently a chemical separation of U from Pu prior to analysis.^{6,7} For ICP-OES, in turn, emission wavelengths of U and Pu might be far away from each other, allowing for an accurate quantification of Pu in samples containing high amounts of U without the need of a chemical separation of Pu prior to analysis.

Previous ICP-OES studies on the determination of Pu investigated either only two^{9,10} or just a few Pu emission wavelengths.^{8,19–21} This restriction limited the chances of identifying suitable Pu emission wavelengths that are free from spectral interferences originating from concomitant elements such as Am, Np, U, and Th that are possibly present at elevated concentrations in the analyte solution. Using an ICP-optical emission spectrometer having a spectral resolution of 20 pm, Claudon *et al.*,⁸ for example, excluded the four prominent Pu emission wavelengths $\lambda = 293.912$ nm, $\lambda = 297.251$ nm, $\lambda =$

298.023 nm, and $\lambda = 299.409$ nm because the Pu signals overlapped with intensive emission wavelengths of Am. Among the remaining Pu emission wavelengths, $\lambda = 453.615$ nm was found to be the most suitable one, tolerating even a ten-fold excess of U relative to Pu.⁸ In the same vein, another more recent study¹⁰ also favoured the Pu emission wavelength at $\lambda = 453.615$ nm over that at $\lambda = 300.057$ nm being less prone to spectral interferences.

To set the above mentioned facts into perspective, one should mention that typical UO_2 -based spent fuels contain ~ 1 mass% of Pu and 96 mass% of U. In mixed oxide (MOX) fuels the amount of PuO_2 can reach up to 30%. While metallic fuels consist of ~ 60 mass% U and ~ 20 mass% Pu, thorium-based (Th, Pu) O_2 fuels may comprise 1.7 mass% U, 0.6 mass% Pu and 83 mass% Th.²²

To shed more light on the potential impact of concomitant elements such as U and Th on Pu ICP-OES analysis, an extensive interference study was carried out. Because of its relevance to reprocessing experiments, the impact of excess amounts of Al, K, Li, Zr and Nd (as a typical representative for fission products) on the Pu ICP-OES signal was also tested. To this end emission spectra of both synthetic standard solutions and actual sample solutions were recorded at the 27 Pu emission wavelengths listed in Table 2.

Part 1 of the interference study, employing standard solutions containing either $0.5 \text{ mg kg}^{-1} \text{ }^{241}\text{Am}$ or 1 mg kg^{-1} of each Pu, U, Th, and ^{237}Np , excluded further potential Pu emission wavelengths. Among them was the Pu emission line at $\lambda = 293.912$ nm, as showcased in Fig. 2. While the presence of Th and ^{237}Np did not spectrally interfere with the Pu emission signal, small amounts of U and particularly Am hampered the reliable determination of Pu at this sensitive Pu emission wavelength (Fig. 2). The presence of Th gave rise to a peak overlapping with the Pu ICP-OES signal at $\lambda = 319.844$ nm, for example, also excluding this emission wavelength for Pu analysis (data not shown).

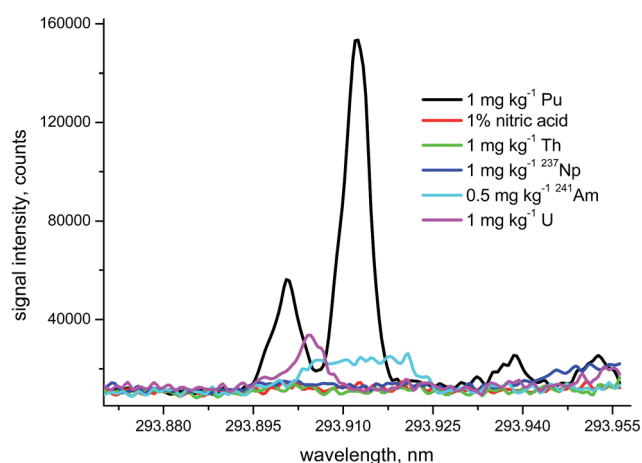


Fig. 2 High resolution ICP-OES spectrum of 1 mg kg^{-1} Pu centred around $\lambda = 293.912$ nm showcasing the impact of $0.5 \text{ mg kg}^{-1} \text{ }^{241}\text{Am}$, and 1 mg kg^{-1} of each ^{237}Np , Th, and U. Each displayed spectrum comprises 101 data points recorded in 1 pm increments.



For part 2 of the interference study, four samples representing a variety of matrix compositions from in-house pyrochemical experiments were selected. Based on the emission spectra recorded for these samples at the 27 wavelengths above, the list of “useful” Pu emission wavelengths was further cut down to the seven wavelengths listed in Table 3. This decision was based on the fact that additional severe spectral interferences occurring at the majority of these 27 emission wavelengths – that were not obvious in the preliminary interferences check using standard solutions (see above) – hampered the reliable determination of Pu. Fig. 3 exemplifies these findings for a set of four samples originating from different steps of pyrochemical separation experiments as observed around one of the most popular Pu emission wavelength, *i.e.* $\lambda = 300.057$ nm. While the reason for the deteriorating peak shape for samples A18 and A32 have not been investigated in detail, the elevated (up to 20 \times) U concentration relative to their Pu amount might be the respective cause. For samples A16 and A30, in turn, Pu emission spectra revealed no spectral interferences around the peak maximum (Fig. 3). Even though being one of the most popular Pu emission lines, $\lambda = 300.057$ nm was not considered for quantification of the element in the investigated nuclear samples because of its incongruous spectral behaviour.

Pu concentration analysis of nuclear samples

External calibration was used for quantification of Pu with ICP-OES in nine nuclear samples (Table 3). The results of 12 replicate analyses (3 replicates each on 4 days) revealed a high reproducibility of the measurements at each of the seven employed Pu emission wavelengths, *i.e.* relative standard deviations (RSD) of ~ 2 –4%. While the majority of the Pu concentrations obtained at the seven emission wavelengths were very similar, however, some discrepancies were also evident. Compared to the other five Pu emission wavelengths calculated Pu concentrations were systematically lower at $\lambda = 390.721$ nm and $\lambda = 439.645$ nm in samples 1 to 5 (Table 3). Similarly, signal intensities recorded at both $\lambda = 299.409$ nm and $\lambda = 299.649$ nm resulted in elevated Pu concentrations for samples 8 and 9. For samples 6 and 7, in turn, high Pu concentrations were obtained

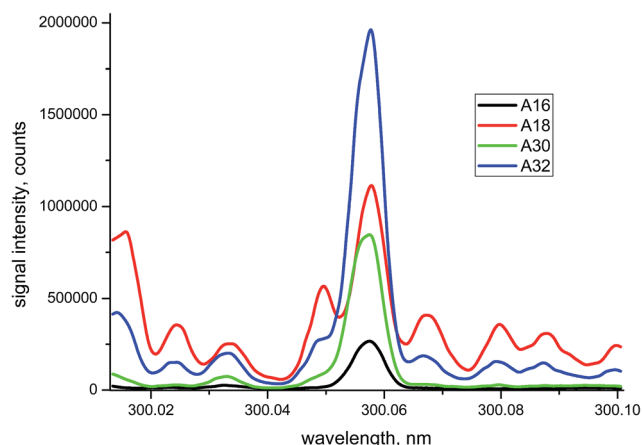


Fig. 3 High resolution ICP-OES spectra of four nuclear samples related to pyrochemical experiments highlighting the extent of potential spectral interferences deteriorating the reliable determination of Pu at one of the most popular Pu emission wavelengths, *i.e.* $\lambda = 300.057$ nm. Each displayed spectrum comprises 101 data points recorded in 1 pm increments. Denomination of samples refers to internal laboratory numbers.

at $\lambda = 299.409$ nm, $\lambda = 299.649$ nm and $\lambda = 390.721$ nm as well as marginally diminished values at $\lambda = 439.645$ nm (Table 3). Spectral interferences of concomitant elements either overlapped partly with the Pu emission signal or slightly increased the spectral background leading to these deteriorating results discussed above.

As a consequence of these experimental facts and to have a single robust set of identical acquisition parameters, only the three Pu emission wavelengths at $\lambda = 297.251$ nm, $\lambda = 449.378$ nm and $\lambda = 453.615$ nm (Table 3) were considered for a reliable quantification of Pu. The selection of these three Pu emission wavelengths for calculating Pu concentrations was additionally supported by the results obtained through replicate standard addition experiments ($N = 12$) carried out with all nine investigated nuclear samples (Table 4).

As no certified matrix-matched reference materials are available for quality assurance, the use of a complementary

Table 3 Concentration of Pu [$N = 12$, mg kg $^{-1}$] in nine sample solutions from pyrochemical experiments obtained at nine ICP-OES emission wavelengths on four consecutive days using external calibration^a

Sample	Emission wavelength, nm						
	297.251	299.409	299.649	390.721	439.645	449.378	453.615
1	0.45 \pm 0.01	0.46 \pm 0.01	0.45 \pm 0.01	0.42 \pm 0.01	0.43 \pm 0.01	0.47 \pm 0.01	0.46 \pm 0.02
2	0.48 \pm 0.01	0.48 \pm 0.01	0.48 \pm 0.01	0.44 \pm 0.00	0.45 \pm 0.01	0.48 \pm 0.02	0.47 \pm 0.02
3	0.43 \pm 0.01	0.42 \pm 0.01	0.43 \pm 0.01	0.39 \pm 0.01	0.42 \pm 0.00	0.46 \pm 0.01	0.42 \pm 0.01
4	0.46 \pm 0.01	0.48 \pm 0.01	0.48 \pm 0.01	0.44 \pm 0.00	0.43 \pm 0.01	0.47 \pm 0.01	0.47 \pm 0.02
5	0.49 \pm 0.01	0.50 \pm 0.00	0.49 \pm 0.01	0.46 \pm 0.00	0.46 \pm 0.01	0.49 \pm 0.01	0.50 \pm 0.02
6	0.55 \pm 0.01	0.80 \pm 0.00	0.95 \pm 0.03	0.68 \pm 0.01	0.51 \pm 0.01	0.54 \pm 0.01	0.54 \pm 0.01
7	0.47 \pm 0.01	0.58 \pm 0.00	0.63 \pm 0.02	0.53 \pm 0.01	0.46 \pm 0.01	0.47 \pm 0.02	0.48 \pm 0.02
8	0.41 \pm 0.01	0.44 \pm 0.00	0.44 \pm 0.01	0.41 \pm 0.01	0.41 \pm 0.01	0.40 \pm 0.01	0.42 \pm 0.01
9	0.51 \pm 0.02	0.57 \pm 0.01	0.59 \pm 0.01	0.53 \pm 0.01	0.51 \pm 0.01	0.51 \pm 0.01	0.53 \pm 0.02

^a Numbers in *italics* indicate results that indicate either diminished or elevated values compared to Pu concentrations obtained at $\lambda = 297.251$ nm, $\lambda = 449.378$ nm and $\lambda = 453.615$ nm. See text for details.



Table 4 Comparison of Pu concentrations [mg kg^{-1}] in nine sample solutions from pyrochemical experiments obtained using ICP-OES and SF-ICP-MS^d

Sample	ICP-OES				SF-ICP-MS bias ^c	
	Standard addition ^a	RSD, %	External calibration ^b	RSD, %	Absolute, mg kg^{-1}	Relative, %
1	0.45 ± 0.02	3.9	0.46 ± 0.01	2.1	-0.02	-4.8
2	0.48 ± 0.01	1.8	0.47 ± 0.01	1.3	-0.04	-8.6
3	0.45 ± 0.02	3.9	0.43 ± 0.02	4.7	-0.04	-8.4
4	0.45 ± 0.00	0.7	0.47 ± 0.01	1.4	0.00	0.0
5	0.47 ± 0.00	0.9	0.50 ± 0.01	1.7	-0.00	-0.1
6	0.54 ± 0.01	2.2	0.54 ± 0.00	0.7	0.00	0.9
7	0.47 ± 0.00	0.4	0.47 ± 0.01	1.2	0.00	0.4
8	0.39 ± 0.01	1.3	0.41 ± 0.01	2.1	-0.01	-2.0
9	0.50 ± 0.01	1.8	0.52 ± 0.01	1.8	0.00	0.4

^a Standard addition experiments using three aliquots of the actual sample and three spiked solutions for each sample aliquot on three consecutive days ($N = 9$). ^b External calibration experiments carried out on four consecutive days ($N = 12$). ^c Difference between the ICP-OES results (based on external calibration) in column 4 and comparative SF-ICP-MS data acquired in-house. Measurement uncertainties of SF-ICP-MS data are $<1\%$. ^d Reported ICP-OES values represent the grand average (and the corresponding standard deviation) calculated from the average Pu concentrations obtained at the three Pu emission wavelengths $\lambda = 297.251 \text{ nm}$, $\lambda = 449.378 \text{ nm}$ and $\lambda = 453.615 \text{ nm}$ (see Table 3).

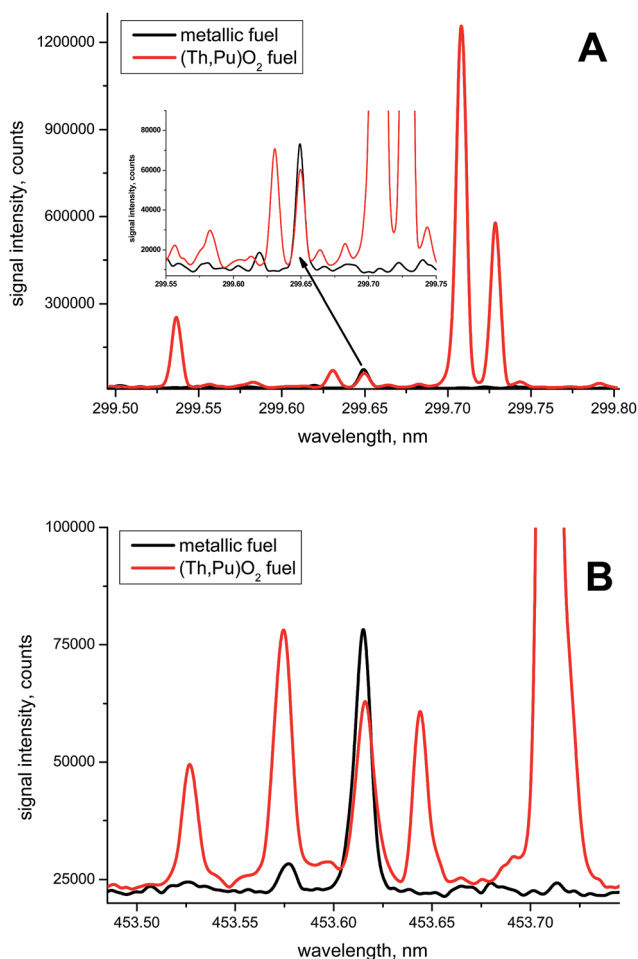


Fig. 4 Smoothed high resolution ICP-OES spectra of solutions of spent, non-separated metallic and $(\text{Th}, \text{Pu})\text{O}_2$ fuels. (A) Emission spectrum centred around $\lambda = 299.649 \text{ nm}$. Insert shows a close-up of the central part of the spectrum. (B) Emission spectrum centred around $\lambda = 453.615 \text{ nm}$. See text for details.

analysis technique whose detection is based on a different physical principle is desirable.¹⁴ To further underpin the accuracy of the selected evaluation regime of the ICP-OES measurements, all samples were also analysed using SF-ICP-MS. To this end, an aliquot from the identical solution that has been used for ICP-OES analysis was also subjected to SF-ICP-MS in-house. In general, ICP-MS results agreed well with ICP-OES data within 2% (Table 4). The results of the samples 1–3, however, did not satisfy these criteria as highlighted in Table 4. In particular, ICP-MS results were up to 8.6% lower than corresponding ICP-OES data. The high matrix load of these three samples ($\text{Np } 2\times$; $\text{Nd } 20\times$; $\text{Li } 25\times$; $\text{K } 100\times$; $\text{Cl } 220\times$) and the inferior capability of the ICP-MS to compensate for the resulting signal suppression is the most likely explanation for this obvious discrepancy between the Pu concentrations established with both analytical techniques. Both the standard addition and the external calibration ICP-OES approach, in turn, yielded equivalent results suggesting sufficiently robust ICP-OES measurement conditions. It is worth mentioning that RSDs of replicate measurements also deteriorated slightly for these three samples (Table 4). Taken together, however, the developed ICP-OES approach generates accurate Pu concentration data for the above mentioned nuclear samples, avoiding a laborious and time-consuming separation of the analyte from the matrix.

Within this study also promising preliminary data for two different spent fuels were obtained. The current experiments were limited by the small volume (a few millilitres) of dissolved spent fuel that was available for testing. As such, high resolution spectra were recorded at the seven Pu emission wavelengths selected previously for the above described nuclear samples. Among them, the two Pu lines at $\lambda = 299.649 \text{ nm}$ (Fig. 4A) and $\lambda = 453.615 \text{ nm}$ (Fig. 4B) gave the impression to work best with this type of samples. Even though the metallic spent fuel contained $\sim 60\%$ U, the corresponding emission spectra emerged straightforward (Fig. 4A and B). The spectra of the spent $(\text{Th}, \text{Pu})\text{O}_2$ fuel, in turn, suffered from the signals



originating from the ~83% Th that were present in the non-separated spent fuel solution (Fig. 4A and B). Due to the high resolution capabilities of the employed ICP-OES instrument, however, the Pu emission signals of both spent fuel solutions were well separated from potential spectral interferences. Further in-depth studies will be needed to give more evidence to the potential of HR-ICP-OES for the reliable determination of Pu in such spent fuel solutions.

Acknowledgements

The supply of the employed Pu certified reference material, the preparation of the investigated samples and comparative Pu concentration analysis using SF-ICP-MS by our colleagues B. Lynch, M. Vargas Zunica, P. Souček, and G. Rasmussen at EC-JRC-ITU is greatly appreciated.

References

- 1 J. Silk, Origin of the heavy metals, in *The Big Bang*, W. H. Freeman and company, New York, USA, 1989, pp. 319–340.
- 2 <http://www.world-nuclear.org/info/Nuclear-Fuel-Cycle/Fuel-Recycling/Plutonium/>.
- 3 International safeguards in nuclear facility design and construction, IAEA nuclear energy series, ISSN 1995–7807, NP-T-2.8, Vienna, International Atomic Energy Agency, 2013.
- 4 X. Hou and P. Roos, *Anal. Chim. Acta*, 2008, **608**, 105–139.
- 5 J. Zheng, K. Tagami, S. Homma-Takeda and W. Bu, *J. Anal. At. Spectrom.*, 2013, **28**, 1676–1699.
- 6 F. Luisier, J. Antonio Corcho Alvarado, P. Steinmann, M. Krachler and P. Froidevaux, *J. Radioanal. Nucl. Chem.*, 2009, **281**, 425–432.
- 7 F. Quinto, E. Hrncsek, M. Krachler, W. Shotyk, P. Steier and S. R. Winkler, *Environ. Sci.: Processes Impacts*, 2013, **15**, 839–847.
- 8 X. Claudon, J. C. Birolleau, M. Lavergne, B. Miche and C. Bergey, *Spectrochim. Acta, Part B*, 1987, **42**, 407–411.
- 9 J. Kulkarni, S. K. Thulasidas, N. Goyal, A. G. Page and M. D. Sastry, *Anal. Lett.*, 1990, **23**, 2095–2106.
- 10 S. K. Thulasidas, V. C. Adya, M. Kumar, T. K. Seshagiri and S. V. Godbole, *At. Spectrosc.*, 2011, **32**, 228–233.
- 11 M. Krachler, R. Alvarez-Sarandes and S. Van Winckel, *J. Anal. At. Spectrom.*, 2013, **28**, 114–120.
- 12 M. Krachler, R. Alvarez-Sarandes, P. Souček and P. Carbol, *Microchem. J.*, 2014, **110**, 425–434.
- 13 M. Krachler, R. Alvarez-Sarandes, P. Carbol, R. Malmbeck and S. Van Winckel, *Microchem. J.*, 2013, **110**, 425–434.
- 14 M. Krachler, R. Alvarez-Sarandes and S. Van Winckel, *J. Radioanal. Nucl. Chem.*, 2015, **304**, 1201–1209.
- 15 P. Souček, R. Malmbeck, C. Nourry and J.-P. Glatz, *Energy Procedia*, 2011, **7**, 396–404.
- 16 S. Van Winckel, L. Aldave de las Heras, P. Carbol, E. Hrncsek, R. Malmbeck, P. Van Belle, E. Zuleger and J.-P. Glatz, LWR-Deputy Project: Radiochemical analysis of a high burn-up (Th,Pu)O₂ sample, irradiated in KWO Obrigheim, *JRC Scientific and Technical Reports*, JRC-ITU-TPW-2010/03, confidential, European Commission, 2010.
- 17 D. Papaioannou, M. Ougier, V. V. Rondinella, J.-P. Glatz and H. Ohta, Post-Irradiation Examinations (PIE) on the U-Pu-Zr Metal Alloy Fuel Rods from the METAPHIX-1 Experiment, *JRC Scientific and Technical Reports*, JRC-ITU-TPW-2010/04, confidential, European Commission, 2010.
- 18 M. Krachler and D. H. Wegen, *J. Anal. At. Spectrom.*, 2012, **27**, 335–339.
- 19 E. Mainka, H. G. Müller and F. Geyer, *Report KfK 3578 (in German)*, "Versuche zur Pu-Bestimmung mit Hilfe der ICP-Methode", Kernforschungszentrum Karlsruhe, Institut für Radiochemie, Karlsruhe, Germany, 1983.
- 20 M. C. Edelson, E. L. DeKalb, R. K. Winge and V. A. Fassel, *Spectrochim. Acta, Part B*, 1986, **41**, 475–486.
- 21 E. A. Huff and D. L. Bowers, *Appl. Spectrosc.*, 1990, **44**, 728–729.
- 22 M. Krachler, R. Alvarez-Sarandes and S. Van Winckel, *J. Anal. At. Spectrom.*, 2014, **29**, 817–824.

